

Iterative Ensemble Kalman Filters for Data Assimilation

Gaoming Li, SPE, and Albert C. Reynolds, SPE, University of Tulsa

Summary

The ensemble Kalman filter (EnKF) is a subject of intensive investigation for use as a reservoir management tool. For strongly nonlinear problems, however, the EnKF can fail to achieve an acceptable data match at certain times in the data assimilation process. Here, we provide two iterative EnKF procedures to remedy this deficiency and explore the validity of these iterative methods compared to the standard EnKF by considering two examples. In both examples, we are able to obtain better data matches using iterative methods than with the standard EnKF.

The simplest derivation of the EnKF analysis equation “linearizes” the objective function by adding the vector of predicted data to the original combined state vector of model parameters and dynamical variables. We show that there is no assurance that this trick for turning a nonlinear problem into a linear problem results in a correct sampling of the probability density function (pdf) one wishes to sample. However, we show that augmenting the state vector with the data results in a correct procedure for sampling the pdf if, at every data assimilation step, the predicted data vector is a linear function of the combined (unaugmented) state vector. Without this assumption, we know of no way to show EnKF samples correctly.

Introduction

The Kalman filter (Kalman 1960) provides an estimate of the state of a linear dynamical system from a sequence of noisy measurements. For a discrete linear dynamical system, the Kalman filtering equations can be derived using the orthogonal projection lemma, as the solution of a sequence of least squares problems or as a minimum variance filter (see Chapter 7 of Jazwinski 1970). Using a Bayesian framework, it is also shown by Jazwinski that for a linear dynamical system with Gaussian errors and a normally distributed initial state, the mean and covariances generated from the Kalman filter are identical to those obtained from the maximum likelihood estimator.

The extended Kalman filter and the iterated Kalman filter were developed for application to nonlinear systems. As shown by Bell and Cathey (1993), the extended Kalman filter is equivalent to the results obtained at the first iteration of the iterated Kalman filter and both reduce to the Kalman filter when the observation function is affine. This result assumes that a prior Gaussian distribution for the current state and normally distributed measurement errors. Although the extended Kalman filter has been used in many applications, because it ignores higher statistical moments, it can yield a poor approximation to the error covariance for highly nonlinear problems. As the error covariance evolves with time, it is possible that the evolutionary equation for the covariance may be unstable (Evensen 2007). Bell and Cathey (1993) provide an example where the state estimated from the extended Kalman filter yields a biased estimate while the updated covariance matrix converges to the null matrix as the measurement error goes to zero. For the same example, the iterated Kalman filter becomes closer to the true state as the measurement error is decreased.

Bell and Cathey (1993) also show that the iterated Kalman filter is equivalent to the Gauss-Newton method for constructing

the maximum likelihood estimate. Their formulation of the maximum likelihood function assumes that an estimate of the state is available, that the true state is normally distributed about this estimate, and that measurement errors are Gaussian with zero means. Variational methods, which led to the 3D variational data assimilation (3D-Var) (Parrish and Derber 1992) and 4D variational data assimilation (4D-Var) methods (Courtier et al. 1994) for weather prediction, appeared before 1990 (Lewis and Derber 1985; Dimet and Talagrand 1986). The 3D-Var method is formulated to maximize the same likelihood function considered by Bell and Cathey (1993). However, for each iteration of the minimization algorithm, the change in the state is usually approximated in a space of lower dimension than the dimension of the state vector. Iteration is typically done with a conjugate gradient or quasi-Newton scheme with the gradient of the cost (objective) function obtained using an adjoint calculation based on a linearization of the observational operator (data functional) about the initial guess, which is normally the background state. The background state represents the best estimate of the state at the current time before assimilating the observations at the current time. In 3D-Var, the background state at the current time is usually the result of a short-range forecast, and, in 4D-Var, the background state may be the result of the previous 4D-Var data assimilation. With the 3D-Var, the observations assimilated are all at the same time, whereas, in 4D-Var, observations with a short time window are assimilated concurrently to obtain an estimate of the initial state, which here is defined as the state at the beginning of the observational time window. Both methods require the minimization of a cost function using a gradient based iterative method.

The weather forecasting problem is distinctly different from the problem of conditioning a reservoir model by assimilating production data. First, in the standard reservoir history-matching problem, our primary concern is the modification of reservoir model parameters (e.g., gridblock permeabilities or porosities, depths of fluid contacts, and parameters defining relative permeability curves) to match production data or seismic data (i.e., reservoir history matching is commonly formulated as a parameter estimation problem rather than a problem of estimating state variables such as pressure and saturation distributions). Second, the initial state represents the initial reservoir pressure and fluid distributions that are usually assumed known when using a gradient-based history-matching algorithm, although there are some exceptions (Evensen et al. 2007; Thulin et al. 2007), whereas, in weather forecasting, the initial state is unknown. When the EnKF is used to assimilate production or seismic data, we consider the history-matching problem as a combined state/parameter problem (Evensen 2007) where the reservoir variables such as gridblock rock properties are the parameters and the primary variables output from the reservoir simulator equations are analogous to the state in the weather prediction problem. In this case, however, we not only are interested in a forecast of the state (e.g., pressures and saturations) but also want to ensure that the updated reservoir parameters are statistically consistent with the updated reservoir state (Thulin et al. 2007). If this consistency does not hold, using the analyzed reservoir state for reservoir management decisions is tenuous.

One additional difference between weather forecasting and reservoir forecasting is that weather forecasting works on a scale of hours, whereas we wish to predict reservoir performance on a scale of years, particularly with the current emphasis on life-cycle optimization (Jansen et al. 2005; Brouwer et al. 2004). A one- to five-day forecast of the weather or the global ocean currents has

definite practical value, whereas a few-day forecast of reservoir performance would be useless for life-cycle reservoir management. Because of the short-term nature of weather forecasting, it is feasible to use a linearized approximation (the tangent linear model) of the dynamical system in 4D-Var to make predictions of the state at discrete data observational times in the observational time interval $[t_0, t_n]$. Linearization of the system dynamics makes it easy to compute the gradient of the cost function using the adjoint method. This is somewhat different than using the adjoint method in history matching (Chavent et al. 1975; Chen et al. 1974; Li et al. 2003; Zhang and Reynolds 2002) where one matches all available data with fixed known initial conditions with the dynamical system for data predictions represented by the full nonlinear system of discretized flow equations.

The problem with the iterated ensemble filter is that each iteration requires the calculation of the gradient of the measurement function (i.e., calculation of the sensitivity matrix). However, this can be avoided by using a quasi-Newton method so one needs only to generate one adjoint solution to compute the gradient of the cost function being minimized. In fact, the iterative method of Zupanski (2005), avoids any formal adjoint solution by exploiting the fact that the sensitivity matrix times a column of the square root of the forecast covariance can be approximated as the difference of two vectors propagated with the full nonlinear dynamics. Despite the additional costs associated with any iterative filter, iteration is often necessary for strongly nonlinear problems to obtain a forecast in reasonable agreement with observations.

The EnKF has been shown to give acceptable history matches and uncertainty predictions for field and pseudofield cases (Evensen et al. 2007; Nævdal et al. 2005; Gu and Oliver 2005; Skjervheim et al. 2006; Gao et al. 2006). The accuracy and reliability of the EnKF itself, however, is not guaranteed because it can yield an incorrect characterization of uncertainty of multimodal problems and a poor match of data for highly nonlinear problems (Zafari and Reynolds 2007; Reynolds et al. 2006; Zhao et al. 2008b). Here, we present two new iterative methods for generating an ensemble of realizations at data assimilation times where the standard EnKF implementation fails to give a reasonable data match. The methods are based on a combination of randomized maximum likelihood (RML) and EnKF methods and are effectively an ensemble RML method. In IEnKF(1), we simply match data sequentially in time as in the normal EnKF procedure. However, we iterate using a gradient-based algorithm to obtain a better match of data than can be obtained by EnKF. Each iteration requires a forward run from time zero and an adjoint solution from the current data assimilation time back to time zero. When this method is employed, the problem is converted to a parameter estimation or sampling problem rather than a combined parameter and state estimation problem. IEnKF(1) is reminiscent of the iterated Kalman filter (Bell and Cathey 1993; Jazwinski 1970) as well as the iterative maximum likelihood ensemble filter (MLEF) method of Zupanski (2005) with some key differences: (1) IEnKF(1) becomes a parameter estimation problem rather than a state estimation problem solved with the iterated Kalman filter; (2) the sensitivity matrix needed is not computed, but we compute the gradient of the cost function with an adjoint method; (3) we generate multiple realizations of the model parameters with each realization updated separately using a Gauss-Newton-type iterative procedure but with a fixed Hessian so our procedure can sample from multiple modes, where, as noted in Zupanski (2005), the iterative Kalman filter and MLEF are not expected to yield multimodal distributions; (4) similar to MLEF but different from the iterated Kalman filter, covariances are represented with a finite ensemble; and (5) at a particular data assimilation time, an approximation of the inverse Hessian matrix is generated only once.

Each iteration of the second iteration scheme, IEnKF(2), presented here, simply requires a forward run from the previous data assimilation time to the current data assimilation time and an adjoint solution from the current data assimilation time back to the previous data assimilation time. While this last iterative scheme is far more efficient than the first one, it requires iteratively updating the primary variables of the reservoir simulator

at the previous data assimilation time. It is conceivable that this could lead to highly nonphysical values, which could introduce errors into our estimates. However, our experiments to date show that this highly efficient method gives fairly reasonable results, but independent testing by other researchers is needed. Note that this second iterative method is somewhat similar to 4D-Var modified for application to a combined parameter and state estimation problem. Unlike 4D-Var, which estimates the initial state at the beginning time t_1 of an observational interval $[t_1, t_n]$ using several data points at discrete times within the interval, IEnKF(2) uses only data at the first observation time t_2 subsequent to t_1 to update model parameters (e.g., gridblock permeabilities and porosities) and dynamic variables (e.g., pressures and saturations) at time t_1 using an iterative procedure. As in EnKF, an ensemble of realizations is updated. After convergence, the forward model (e.g., the reservoir simulator) is run forward from t_1 (not from time zero) to t_2 and to the next data assimilation time (t_3) for each updated realization of parameters and dynamic variables. As in EnKF, this set of predictions at t_2 represents the "prior model" at t_2 , which is then updated by assimilating data at the observational time after t_3 .

The application of EnKF to reservoir simulation problems assumes that predictions of primary variables are made forward in time and that the last updated (analyzed) ensemble of reservoir parameters and simulation primary variables is statistically consistent with those made from time zero using the ensemble of reservoir parameters obtained at the last data assimilation step. Predicting forward from the last data assimilation is far more computationally efficient, but rerunning from time zero has the advantage that we avoid nonphysical values of pressure and saturation at all timesteps and maintain material balances. The hope is that the two methods will give similar results in terms of the estimate of the mean prediction and uncertainty. In some cases, this is true, but, in others, the two sets of results can be radically different (Zhao et al. 2008a). For a linear problem with no model error, a Gaussian prior model, and uncertain initial conditions, Thulin et al. (2007) have shown that predictions from time zero with the final ensemble of the vector of model parameters and updated initial conditions have the same expectation and covariance as are obtained by running forward from the last data assimilation step. Similarly, Zafari and Reynolds (2007) have shown that, for a linear problem with a Gaussian prior and no model error, the EnKF becomes equivalent to RML as the ensemble size goes to infinity. Thus, in this situation, EnKF samples the correct pdf, at least asymptotically, a result that also can be found in Evensen (2007). For the same situation, the same method can be used to show the iterative methods given here sample the pdf (Eq. 4) correctly as the ensemble size goes to infinity. While this is comforting, there is no guarantee the methods sample the pdf correctly for nonlinear, non-Gaussian problems.

Problem Formulation as a Conditional PDF

The N_m -dimensional column vector of model parameters is denoted by m . Model parameters can include reservoir gridblock permeabilities and porosities, fault transmissibilities, fluid contacts, initial fluid distributions, or parameters describing relative permeabilities, but, in the examples presented here, only porosities and log-permeabilities are included as model parameters. We let t_n , $n = 1, 2, \dots$, denote the simulation time steps with $t_0 = 0$ and let the random N_p -dimensional column vector p^n denote the vector of dynamical variables (i.e., the primary variables of the reservoir simulation equations at time t_n , where p^0 denotes the random vector that represents the initial conditions. For a black-oil system, p^n includes reservoir gridblock pressures, saturations and solution gas/oil ratios. Note that the random vector p^n depends on time but m (i.e., the N_m -dimensional random column vector of model parameters) does not. However, the joint conditional pdf for these random vectors evolves in time as more data are assimilated. Here, we assume that model error is negligible. Boundary conditions are also assumed known. In the development of the specific Gaussian forms of the pdf, we assume that the initial state (p^0) is a random vector with Gaussian statistics and independent of the vector of model parameters m .

The vector d^n represents the N_n -dimensional random column vector of predicted data at time t_n , $n = 1, 2, \dots$, where these times denote the times at which we wish to assimilate data (i.e., condition m and p^n) to observations, d_{obs}^n . The N_n -dimensional column vector of predicted data at the n th data assimilation step (time t_n) is denoted by

$$d^n = g_n(m, p^n) = g_n(y^n), \dots \quad (1)$$

where the $N_y = N_m + N_p$ -dimensional column vector, y^n , is given by

$$\begin{bmatrix} m \\ p^n \end{bmatrix} = \begin{bmatrix} m^n \\ p^n \end{bmatrix}. \dots \quad (2)$$

In the last expression, we have put a superscript n on m simply to denote that we are focusing on conditioning m to data at the n th data assimilation step, which corresponds to time t_n . Note y^n contains both information on the state of the reservoir system and the reservoir model parameters, but we will simply refer to y^n as the state vector at t_n . Here, for simplicity in notation, we have assumed that data assimilation steps coincide with reservoir simulator timesteps, but no theoretical or practical problems arise when data are assimilated at a subset of the simulation time steps (Evensen 2007; Li and Reynolds 2007).

This paragraph summarizes well-known historical results that can be found in Evensen (2007). Assuming that measurement errors at any two distinct data assimilation times are independent, it can be shown using Bayes theorem that the pdf for y^n conditional to all data at times up to and including those at t_n is given by

$$\begin{aligned} f(y^n | d_{\text{obs}}^n, \dots, d_{\text{obs}}^1) \\ = af(d_{\text{obs}}^n | y^n) f(y^n | d_{\text{obs}}^{n-1}, \dots, d_{\text{obs}}^1), \dots \end{aligned} \quad (3)$$

where a is the normalizing constant and throughout, f always denotes a pdf with the arguments of f used to specify which pdf is represented. A sample of the last pdf on the right-hand side of Eq. 3 can be obtained by propagating a realization of y^{n-1} obtained as a sample of $f(y^{n-1} | d_{\text{obs}}^{n-1}, \dots, d_{\text{obs}}^1)$ forward in time using the reservoir simulation equations, which we assume is a Markov process. The pdf $f(y^n | d_{\text{obs}}^{n-1}, \dots, d_{\text{obs}}^1)$ represents the prior pdf for y^n before assimilating data d_{obs}^n . Note that Eq. 3 is in the form of a general Bayesian updating equation and requires no assumptions of linearity or Gaussianity. We use a superscript p to represent prior (or predicted) and assume this prior is Gaussian with mean $\bar{y}^{n,p}$ and covariance matrix $C_{Y^{n,p}}$. We also assume that the vector of measurement errors at any time t_n is Gaussian with mean zero and covariance C_{D^n} . With the above set of assumptions, Eq. 3 can be written as

$$\begin{aligned} f(y^n | d_{\text{obs}}^n, \dots, d_{\text{obs}}^1) = a \exp \left(-\frac{1}{2} \left[y^n - \bar{y}^{n,p} \right]^T C_{Y^{n,p}}^{-1} \left[y^n - \bar{y}^{n,p} \right] \right. \\ \left. - \frac{1}{2} \left(d^n - d_{\text{obs}}^n \right)^T C_{D^n}^{-1} \left(d^n - d_{\text{obs}}^n \right) \right), \dots \end{aligned} \quad (4)$$

which represents the pdf we wish to sample. Using the definition of y^n , Eq. 4 is equivalent to

$$\begin{aligned} f(y^n | d_{\text{obs}}^n, \dots, d_{\text{obs}}^1) \\ = f(m^n, p^n | d_{\text{obs}}^n, \dots, d_{\text{obs}}^1) = a \exp \left(-\frac{1}{2} \left[\begin{bmatrix} m^n - \bar{m}^{n,p} \\ p^n - \bar{p}^{n,p} \end{bmatrix} \right]^T \right. \\ \left. C_{Y^{n,p}}^{-1} \left[\begin{bmatrix} m^n - \bar{m}^{n,p} \\ p^n - \bar{p}^{n,p} \end{bmatrix} \right] - \frac{1}{2} \left(d^n - d_{\text{obs}}^n \right)^T C_{D^n}^{-1} \left(d^n - d_{\text{obs}}^n \right) \right). \dots \end{aligned} \quad (5)$$

From the viewpoint of inverse theory, Eq. 4 or, equivalently, Eq. 5 defines the solution of the problem, but practically, to evaluate uncertainty, we wish to generate a set of samples of this pdf. RML provides one way to generate an approximate sampling of this pdf; other methods are described by Oliver et al. (2008). When predicted data are linearly related to model parameters, the pdf in Eq. 4 is Gaussian; moreover, RML and EnKF become equivalent and both methods provide a correct procedure to sample the pdf (Evensen 2007; Zafari and Reynolds 2007).

EnKF Analysis Equation. The derivation of the EnKF for a nonlinear data functional can be done conveniently by adding predicted data to the original state vector to obtain the augmented state vector defined by

$$\tilde{y}^n = \begin{bmatrix} y^n \\ d^n \end{bmatrix} = \begin{bmatrix} m^n \\ p^n \\ d^n \end{bmatrix}. \dots \quad (6)$$

for $n = 1, 2, \dots$, (Evensen 2003). Then, analogous to Eq. 3, we obtain the pdf

$$\begin{aligned} f(\tilde{y}^n | d_{\text{obs}}^n, \dots, d_{\text{obs}}^1) = af(d_{\text{obs}}^n | \tilde{y}^n) f(\tilde{y}^n | d_{\text{obs}}^{n-1}, \dots, d_{\text{obs}}^1), \\ \dots \end{aligned} \quad (7)$$

where again we assume measurement errors at different data assimilation times are independent.

Recall that the column vectors m^n , p^n , and d^n , respectively, have dimensions N_m , N_p , and N_n . Letting

$$H = \begin{bmatrix} O & I_{N_n} \end{bmatrix}, \dots \quad (8)$$

where O is the $N_n \times (N_m + N_p)$ null matrix and I_{N_n} is the $N_n \times N_n$ identity matrix, we see that

$$d^n = H\tilde{y}^n. \dots \quad (9)$$

So, by the “trick” of adding d^n to the state vector, we have a linear relation between the random data vector d^n and the augmented state vector \tilde{y}^n .

As in the derivation of Eq. 4, we assume that the dynamical system is a Markov process, that the “prior” pdf on the right-hand side of Eq. 7 is Gaussian with mean $\bar{y}^{n,p}$ and covariance matrix $C_{\tilde{Y}^{n,p}}$, and that measurement error at any t_n is Gaussian with mean zero and covariance C_{D^n} . With these assumptions, the pdf of Eq. 7 can be written in the form of Eq. 4 with y replaced by \tilde{y} and is given by

$$\begin{aligned} f(\tilde{y}^n | d_{\text{obs}}^n, \dots, d_{\text{obs}}^1) = a \exp \left(-\frac{1}{2} \left(\tilde{y}^n - \bar{y}^{n,p} \right)^T C_{\tilde{Y}^{n,p}}^{-1} \left(\tilde{y}^n - \bar{y}^{n,p} \right) \right. \\ \left. - \frac{1}{2} \left(H\tilde{y}^n - d_{\text{obs}}^n \right)^T C_{D^n}^{-1} \left(H\tilde{y}^n - d_{\text{obs}}^n \right) \right). \dots \end{aligned} \quad (10)$$

Because of the linearity of the operator H and the assumption that the prior is Gaussian, the pdf of Eq. 10 can be sampled correctly using RML (Oliver et al. 1996; Reynolds et al. 1999; Oliver et al. 2008). If $\tilde{y}_j^{n,p}$ is a sample of the prior Gaussian pdf for \tilde{y}^n and $d_{\text{uc},j}^n$ is a sample of the Gaussian pdf that has mean d_{obs}^n and covariance C_{D^n} , then a corresponding sample of the pdf of Eq. 10 is given by the RML equation

$$\tilde{y}_j^{n,u} = \tilde{y}_j^{n,p} + C_{\tilde{Y}^{n,p}} H^T \left(C_{D^n} + H C_{\tilde{Y}^{n,p}} H^T \right)^{-1} \left(d_{\text{uc},j}^n - H\tilde{y}_j^{n,p} \right). \dots \quad (11)$$

We can generate realizations of the augmented state vector for $j = 1, 2, \dots, N_e$ by applying this same procedure. This RML equation is identical to the standard EnKF analysis equation (Evensen 2007) except, at this point, we assume we use the full covariance matrix. Because we have included predicted data in the augmented state vector, Eq. 11 also gives an updated data vector, but this is not used in our algorithms, and, effectively, we do not need to compute the data part of the augmented state vector.

With the trick of adding d^n to the state vector, EnKF samples the pdf of Eq. 10 correctly. Although the marginal pdf for y^n obtained from the joint pdf $f(y^n | d_{\text{obs}}^n, \dots, d_{\text{obs}}^1)$ is formally given by $f(y^n | d_{\text{obs}}^n, \dots, d_{\text{obs}}^1)$, it is important to note that we used different Gaussianity assumptions to define precise forms of these two pdfs (see Eqs. 4 and 10). Thus, there is no assurance that the marginal pdf for y^n obtained from Eq. 10 is equal to the pdf on the right side of Eq. 4 derived under different assumptions. The equivalence of these two pdfs can be shown only if the data functional is linear (Li and Reynolds 2007). Thus, in the nonlinear case, there is no assurance that EnKF provides realizations that represent samples of the pdf of Eq. 4. While there may be many causes for poor performance of the EnKF, the iterative methods presented here were designed to improve results when strong nonlinearities make it difficult to obtain a reasonable data match. The first iterative method presented also will alleviate problems caused by inconsistency between the dynamical (primary) and model parameters where consistency is defined by Thulin et al. (2007).

IEnKF(1)

The first iterative method, IEnKF(1), represents a sequential application of RML obtained by using a finite ensemble and some of the EnKF methodology to approximate the Hessian in the Gauss-Newton optimization algorithm. With this iterative method, whenever the standard EnKF update does not provide an acceptable data match, we iterate on the model parameter part of the state vector using an algorithm similar to a quasi-Newton method (Nocedal and Wright 1999) with a fixed Hessian approximation. Note this iterative procedure modifies the state and parameter estimation/sampling problem to a model parameter estimation/sampling problem. In this procedure, the simulation equations are solved from time zero to the current data assimilation step and the gradient needed in a quasi-Newton is computed with the adjoint method. Updated values of the primary variables p^n are computed from the reservoir simulator run from time zero using updated values of the model parameters. With this procedure, we generate a sample of the model part of the pdf of Eq. 5 (i.e., the problem becomes a parameter estimation problem rather than a parameter and state estimation problem). With RML, a sample can be obtained with the following algorithm: Use a Gauss-Newton formula to compute a search direction as

$$\delta m_j^{n,\ell+1} = - \left(C_{M^n} + C_{M^n} G_{n,j,\ell}^T \left(C_{D^n} + G_{n,j,\ell} C_{M^n} G_{n,j,\ell}^T \right)^{-1} G_{n,j,\ell} C_{M^n} \right) \\ \left[C_{M^n}^{-1} \left(m_j^{n,\ell} - m_j^{n,p} \right) + G_{n,j,\ell}^T C_{D^n}^{-1} \left(d^n \left(m_j^{n,\ell} \right) - d_{\text{uc},j}^n \right) \right], \quad (12)$$

where ℓ is the iteration index, and then update the vector of model parameters as

$$m_j^{n,\ell+1} = m_j^{n,\ell} + \alpha_j^{\ell+1} \delta m_j^{n,\ell+1}, \quad (13)$$

where the step size $\alpha_j^{\ell+1}$ is computed by a line search method similar to the one used by Gao and Reynolds (2006). This algorithm represents RML for generating samples of the pdf for m conditional to d_{obs}^n . Here, $G_{n,j,\ell}^T$ denotes the gradient of $(d^n)^T$ with respect to m evaluated at $m_j^{n,\ell}$, and $m_j^{n,p}$ denotes the j th realization obtained by conditioning to data up to and including the $(n-1)$ th data assimilation time. It is important to note that this still represents a sequential data assimilation process in that C_{M^n} represents the prior covariance matrix for m^n , which has the pdf $f(m^n | d_{\text{obs}}^{n-1}, \dots, d_{\text{obs}}^1)$.

In Eq. 12, the matrix

$$\hat{H}_\ell \equiv C_{M^n} + C_{M^n} G_{n,j,\ell}^T \left(C_{D^n} + G_{n,j,\ell} C_{M^n} G_{n,j,\ell}^T \right)^{-1} G_{n,j,\ell} C_{M^n} \dots \quad (14)$$

is the Gauss-Newton inverse Hessian at the ℓ th iteration. We use EnKF methodology to approximate this inverse Hessian as

$$\hat{H}_\ell \approx C_{M^n} + C_{M^n, D^n} \left(C_{D^n} + C_{D^n, D^n} \right)^{-1} C_{D^n, M^n}, \quad (15)$$

where this approximation is also meant to indicate that we will approximate the inverse Hessian using the EnKF methodology with a finite number of ensemble members. This approximation is motivated by the fact established by Reynolds et al. (2006) that $C_{M^n} G_{n,j,\ell}^T$, $G_{n,j,\ell} C_{M^n} G_{n,j,\ell}^T$, and $G_{n,j,\ell} C_{M^n}$, respectively, can be approximated by C_{M^n, D^n} , C_{D^n, D^n} , and C_{D^n, M^n} . With the approximation of Eq. 15, Eq. 12 is replaced by

$$\delta m_j^{n,\ell+1} = - \left(C_{M^n} + C_{M^n, D^n} \left(C_{D^n} + C_{D^n, D^n} \right)^{-1} C_{D^n, M^n} \right) \\ \left[C_{M^n}^{-1} \left(m_j^{n,\ell} - m_j^{n,p} \right) + G_{n,j,\ell}^T C_{D^n}^{-1} \left(d^n \left(m_j^{n,\ell} \right) - d_{\text{uc},j}^n \right) \right]. \quad (16)$$

Except for the fact that we approximate the covariance by a limited ensemble, the terms in braces in Eq. 16 represent the gradient of the objective function

$$O_m(m^n) = \frac{1}{2} \left(\left(m^n - m_j^{n,p} \right)^T C_{M^n}^{-1} \left(m^n - m_j^{n,p} \right) \right. \\ \left. + \left(d^n - d_{\text{uc},j}^n \right)^T C_{D^n}^{-1} \left(d^n - d_{\text{uc},j}^n \right) \right), \quad (17)$$

with respect to m^n evaluated at $m_j^{n,\ell}$. Here we assume C_{D^n} is of full rank so that $C_{D^n}^{-1}$ is well defined. The gradient of the data mismatch part of the objective function, i.e.

$$v_j = G_{n,j,\ell}^T C_{D^n}^{-1} \left(d^n \left(m_j^{n,\ell} \right) - d_{\text{uc},j}^n \right), \quad (18)$$

is calculated using our standard implementation of the adjoint method (Zhang and Reynolds 2002; Gao and Reynolds 2006).

In the preceding iterative EnKF method, the $N_m \times N_m$ model covariance matrix C_{M^n} is represented by the N_e ensemble members and will usually be rank deficient and hence singular. Thus, when we represent C_{M^n} by the ensemble members as is standard in EnKF, the term $w_j \equiv C_{M^n}^{-1} \left(m_j^{n,\ell} - m_j^{n,p} \right)$ in Eq. 16 is calculated by using singular value decomposition (SVD) to solve

$$C_{M^n} w_j = \left(m_j^{n,\ell} - m_j^{n,p} \right). \quad (19)$$

In generating a solution of Eq. 19 by SVD, we do not need to form C_{M^n} explicitly; an SVD of the matrix with the j th column given by $m_j^{n,p} - m_j^{n,\ell}$ is sufficient to generate a solution of Eq. 19.

Note that, at this point, the gradient of the objective function of Eq. 17 is given by $x_j \equiv v_j + w_j$ so Eq. 16 is identical to

$$\delta m_j^{n,\ell+1} = -C_{M^n} x_j - C_{M^n, D^n} \left(C_{D^n} + C_{D^n, D^n} \right)^{-1} C_{D^n, M^n} x_j. \quad (20)$$

Similar to the EnKF method, we approximate covariances involving m^n and d^n using the finite ensemble so that $C_{M^n} x_j$ and $C_{D^n, M^n} x_j$, respectively, are calculated as

$$q_j \equiv C_{M^n} x_j = \frac{1}{N_e - 1} \sum_{k=1}^{N_e} \left(m_k^{n,p} - \bar{m}^{n,p} \right) \left(m_k^{n,p} - \bar{m}^{n,p} \right)^T x_j \quad (21)$$

function (Eq. 29) with respect to y^n evaluated at $y_j^{n,\ell}$. As in the first iterative method, IEnKF(1), the inverse of the Gauss-Newton Hessian matrix is approximated using the EnKF methodology,

$$\begin{aligned} \hat{H}_\ell &\equiv C_{Y^n, p} + C_{Y^n, p} S_{n+1, j, \ell}^T \left(C_{D^{n+1}} + S_{n+1, j, \ell} C_{Y^n, p} S_{n+1, j, \ell}^T \right)^{-1} S_{n+1, j, \ell} C_{Y^n, p} \\ &\approx C_{Y^n, p} + C_{Y^n, p, D^{n+1}} \left(C_{D^{n+1}} + C_{D^{n+1}, D^{n+1}} \right)^{-1} C_{D^{n+1}, Y^n, p}. \end{aligned} \quad \dots \quad (34)$$

Using the approximation of Eq. 34 in Eq. 33, yields,

$$\delta y_j^{n,\ell+1} = - \left(C_{y^n,p} + C_{y^n,p,D^{n+1}} \left(C_{D^{n+1}} + C_{D^{n+1},D^{n+1}} \right)^{-1} C_{D^{n+1},y^n,p} \right) \\ \left[C_{y^n,p}^{-1} \left(y_j^{n,\ell} - y_j^{n,p} \right) + S_{n+1,j,\ell}^T C_{D^{n+1}}^{-1} \left(d^{n+1} \left(y_j^{n,\ell} \right) - d_{\text{uc},j}^{n+1} \right) \right].$$

(35)

Similar to the discussion on the first iterative method, IEnKF(1), the part of the gradient of the objective function represented by $S_{n+1,j,\ell}^T C_{D^{n+1}}^{-1} (d^{n+1}(y_j^{n,\ell}) - d_{\text{obs},j}^{n+1})$ is calculated by the adjoint procedure. But, unlike in the first iterative method, the adjoint is only applied backward from time t_{n+1} to t_n instead of all the way back to time zero. Moreover, instead of computing a gradient of the data mismatch part of the objective function with respect to m and adjusting only m by Gauss-Newton iteration, we adjust m and p^n to match data d_{obs}^{n+1} . The calculation of the adjoint gradient with respect to m and p^n is fairly straightforward and similar to the implementation given by Eydinov et al (2007), where it was necessary to compute the gradient of the objective function with respect to the initial saturation distribution. Once the adjoint gradient is obtained, the rest of the calculation in Eq. 35 is similar to that of Eq. 16 in the first iterative method, IEnKF(1).

As in the first iterative method, we use EnKF without iteration at the n th data assimilation step (time t_n), provided the predicted data at t_n gives a value of the normalized objective function (Eq. 26) less than or equal to 5. When this does not hold, we iterate using IEnKF(2).

Examples

In this section, we compare the performance of the standard and iterative EnKF algorithms for two examples, essentially the same as the ones considered previously by Zafari and Reynolds (2007). The first example is a one-parameter toy problem, and the second one is closer to a realistic reservoir problem.

Toy Problem. Here $p^0 = 1$, $d^n = g_n(m, p^n)$ is identical to p^n and the discrete evolutionary equation is given by

$$d^n = p^n = p^{n-1} - \frac{9\Delta t}{2} \left(m - \frac{2\pi}{3} \right)^2 \dots \dots \dots \quad (36)$$

for $n = 1, 2, \dots$, where $\Delta t = 1$ and $t_0 = 0$. The true data are generated with $m_{\text{true}} = 1.88358$ at five times ($t_j = j$, $j = 1, 2, 3, 4, 5$). Because of the quadratic nature of the problem (Eq. 36), the same true data can be generated with $m = 2.30521$. For each time, synthetic observed data were generated by adding to the true d^n random noise sampled from $N(0, 0.01)$. The initial prior model for m is Gaussian, $m \sim N(2.1, 0.2)$. **Fig. 1a** shows the true posterior pdf for m conditional to the five observed data. The posterior pdf shows two peaks: one approximately at m_{true} and another at $m = 2.3$. The histogram of model parameters after matching the five observed data with RML is shown in Fig. 1b. Note that RML gives an accurate representation of the true pdf of Fig. 1a, which is the pdf we wish to sample. To obtain the RML results of Fig. 1b, we generated 5,000 realizations with RML. In applying IEnKF(1) and IEnKF(2) for this example, we also use an ensemble size of 5,000, where the initial set of realizations is obtained by sampling the prior Gaussian model.

Comparing Fig. 1c with Fig. 1a, we see that standard EnKF provides a poor approximation to the true pdf, whereas the iterative methods give improved approximations (Figs. 1d and 1e) to the true pdf. IEnKF(1) yields a fairly accurate sampling of the true pdf but not as good a representation as obtained with RML, where all data are matched concurrently. IEnKF(1) (Fig. 1d) slightly overpredicts the uncertainty in m because, in assimilating data sequentially, we are still forced to assume the prior at each assimilation step can be approximated by a Gaussian and that the updated

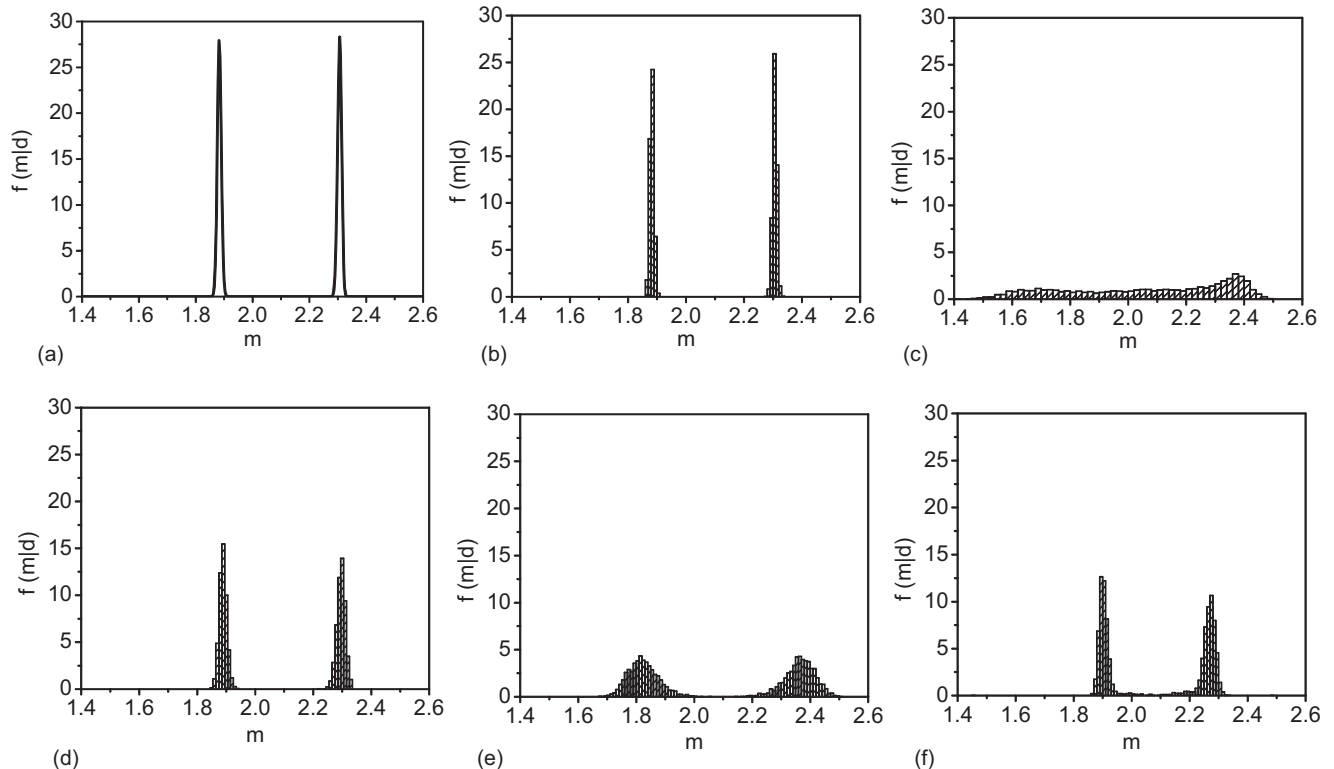


Fig. 1—True (a) and approximate posterior probability density functions, toy problem. (a) Posterior pdf, the fifth datum. (b) RML, the fifth datum. (c) EnKF, the fifth datum. (d) IEnKF(1), the fifth datum. (e) IEnKF(2), the fifth datum. (f) IEnKF, the 20th datum.

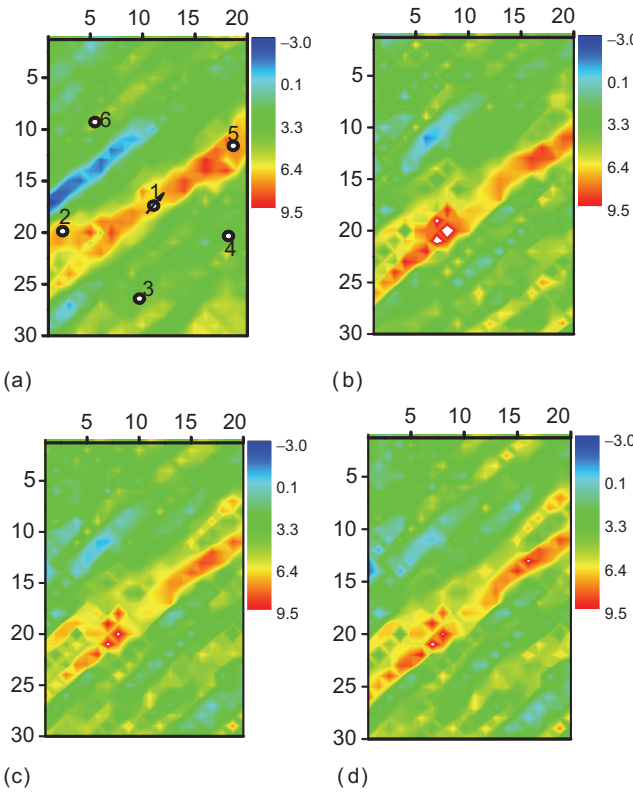


Fig. 2—Horizontal log-permeability. (a) True. (b) Standard EnKF. (c) IEnKF(1). (d) IEnKF(2).

model honors all data assimilated previously. IEnKF(2) (Fig. 1e) overestimates the uncertainty in the model, although it gives a pdf with the two modes in the correct position and gives a much better approximation to the true pdf than the standard EnKF.

As we assimilate more data using IEnKF(2), we obtain a better approximation to the true pdf as illustrated in Fig. 1f. (The true posterior pdf after assimilating 20 data points will still have the two modes at the positions shown in Fig. 1a, and, in fact, the true posterior pdf after assimilating 20 data points is very similar to that shown in Fig. 1a.) On the other hand, the pdf generated by assimilating 20 data points with EnKF does not give a better approximation to the true pdf than was obtained in Fig. 1c.

IEnKF(2) is by far the most efficient iterative EnKF scheme presented in the paper because, at each iteration, it only requires generating the forward and adjoint solution on the interval $[t_{n-1}, t_n]$ when assimilating data at time t_n . However, it generates a less accurate characterization of uncertainty than the first iterative EnKF method. Thus, more studies are needed to carefully delineate its utility for real applications.

Synthetic Reservoir Problem. This example pertains to a 2D horizontal reservoir with a grid system of 20×30 . The size of the reservoir is $6,000 \times 9,000$ feet. A detailed description of the problem can be found in Zafari and Reynolds (2007). The true horizontal log-permeability map with the location of the six wells is shown in **Fig. 2a**. Well 1 is put on production on Day 1 with all the other wells being shut in. Well 2 is then put on production after Well 1 produces for 90 days. The sequence of opening a new well every 90 days continues until all the wells are put on production. Each well is produced at a specified oil rate of $q_o = 100$ STB/D. After Day 540, Well 1 is switched from a producer to a water injector with the water-injection rate set equal to 1,000 STB/D, and, at this time, the rate at all producing wells is increased to $q_o = 200$ STB/D. At Day 5,580, the injection rate for Well 1 is increased to 2,000 STB/D and the oil-production rate for all the producers is increased to 300 STB/D. At Day 5,850, Well 5 is shut in because of a high water/oil ratio (WOR) and all the other wells remain on the previous production schedule until Day 7,290. After data

assimilation up to Day 7,290, we predict the reservoir performance to Day 10,000 by maintaining the injection rate at 2,000 STB/D and setting the bottomhole pressures (BHP) for Well 2, Well 3, Well 4, and Well 6 equal to 2,500 psi, 1,000 psi, 1,500 psi and 300 psi, respectively. Well 5 is kept shut-in.

The observation data in this study include the flowing BHP, producing gas/oil ratio (GOR), and WOR. The true synthetic data are generated with the simulator CLASS (Chevron's Limited Applications Simulation System), and the observation data are obtained by adding Gaussian random noise to the true synthetic data. The random Gaussian noise added is based on standard deviations of 5% for bottomhole flowing pressure and producing GOR, and 0.1% for WOR. The initial prior for m , which consists of gridblock porosities and log-permeabilities is Gaussian; see Zafari and Reynolds (2007) for additional details. In applying the EnKF methods, we use an ensemble size of 90 with the initial suite of models generated from the Gaussian prior.

Because IEnKF(1) requires the gradient of the objective function obtained by running the simulator from time zero to the current data assimilation time and then running the adjoint code back to time zero, it can require considerable computer time if this procedure is applied for all ensemble members at every data assimilation step. To avoid this situation, we apply the iteration procedure only when the normalized objective function (Gao and Reynolds 2006) calculated using predicted data at that assimilation time is greater than 5. We use a simplified version of the Gao and Reynolds (2006) line search procedure. However, we allow only a maximum of five iterations, and this may not be enough for some problems. Data are assimilated sequentially at 90 day intervals to generate updated descriptions of the porosity field and the isotropic permeability field. For comparison purposes, we also apply IEnKF(2) whenever the normalized objective function obtained by the normal EnKF update is greater than 5.

Fig. 2b shows the average log-permeability after assimilating data up to Day 7,290 with the standard EnKF. Figs. 2c and 2d show the average log-permeability after assimilating data up to Day 7,290 with the two iterative EnKF methods. All methods give an average log-permeability field, which shows the basic geological features of the true permeability field (i.e., a visual comparison suggests little improvement was obtained with the iterative EnKF methods).

Figs. 3a, 3c, and 3e show the production predictions by running the simulator forward from the last data assimilation time compared to the predictions from the true model. Note the EnKF predictions for the cumulative oil (Fig. 3a) and water production (Fig. 3c) are biased and do not span the truth and, hence, do not correctly characterize the uncertainty in performance predictions. Although not shown here, the EnKF ensemble predictions of the cumulative gas production are only slightly less biased. The data match during data assimilation and prediction for the producing WOR of Well 2 is shown in Fig. 3e. As we assimilated data up to Day 7,290, this result shows that EnKF did not yield a match of the WOR data; all the ensemble members have later water breakthrough than the true case and give poor predictions until $t > 9,000$ days. This late breakthrough is the reason that EnKF gives a high estimate of cumulative oil production and a low estimate of cumulative water production. Figs. 3b, 3d, and 3f compare the production predictions run from time zero using the final ensemble of models with the predictions from the true model. To obtain these predictions, we ran the simulator from time zero to Day 10,000 using the ensemble obtained after assimilating data up to Day 7,290; these results are even more biased, but the two sets of results are not radically different qualitatively.

Figs. 4a, 4c, and 4e show the future performance predictions obtained by running the simulator forward from the last data assimilation time with IEnKF(1). Figs. 4b, 4d, and 4f show the future performance predictions obtained by running the simulator forward from zero with the final ensemble obtained from IEnKF(1). Compared to the standard EnKF, this iterative EnKF method gives a much more accurate estimate of the true future performance prediction and appears to give a reasonable characterization of the uncertainty in predictions; but, the last state-

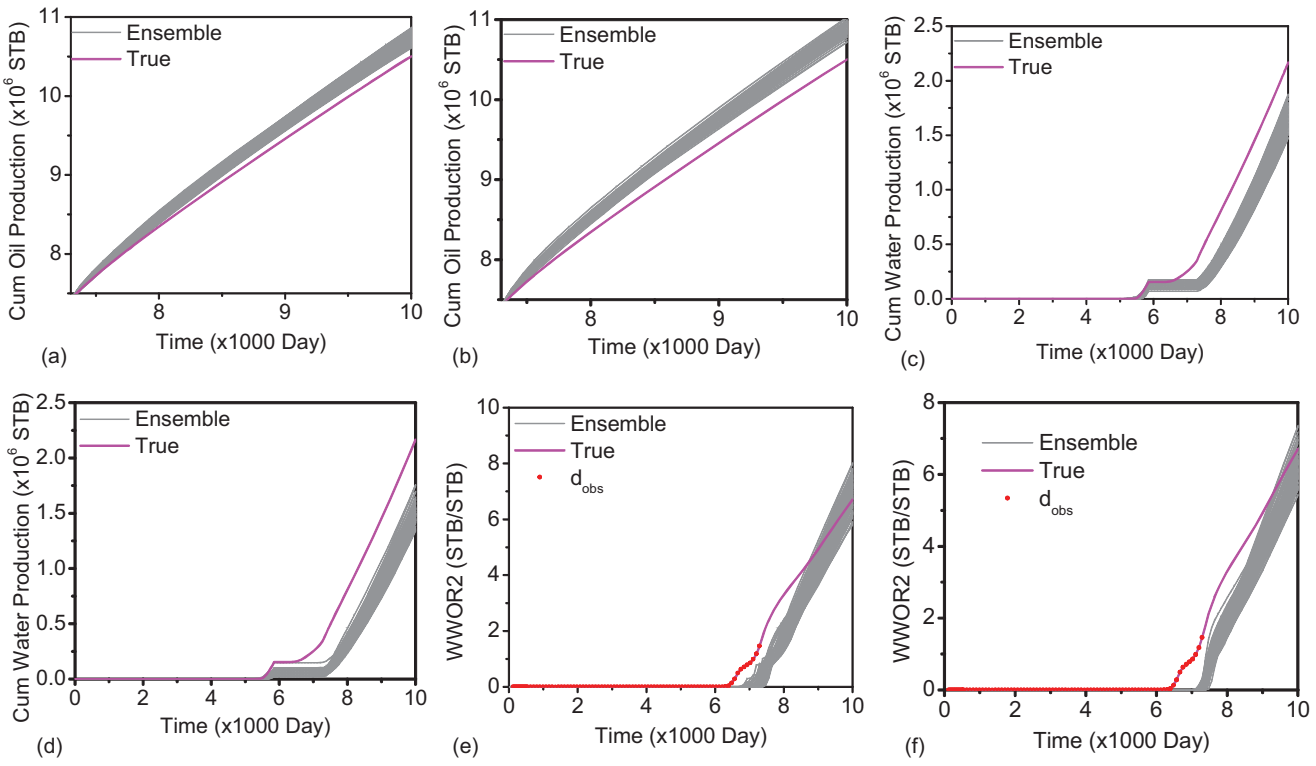


Fig. 3—Production predictions with standard EnKF during data assimilation (a, c, and e) and predicted from Time 0 (b, d, and f).

ment can not be verified without an exhaustive sampling of the true posterior pdf, which is not feasible. Figs. 4c and 4d show a staircase increase in the cumulative water production. The water production of the first stage comes from Well 5, the flat part on the curves corresponds to times when Well 5 is shut in but water breakthrough has not occurred at Well 2. The cumulative water production before the horizontal section (Fig. 4c) shows an almost

exact agreement between the ensemble and the truth, which occurs because this iterative EnKF method matches the WOR data of Well 5 (not shown) almost exactly.

Figs. 5a, 5c, and 5e shows the future performance predictions obtained by running the simulator forward from the last data assimilation time with IEnKF(2). Better future performance predictions are obtained compared to the standard EnKF, but the results are

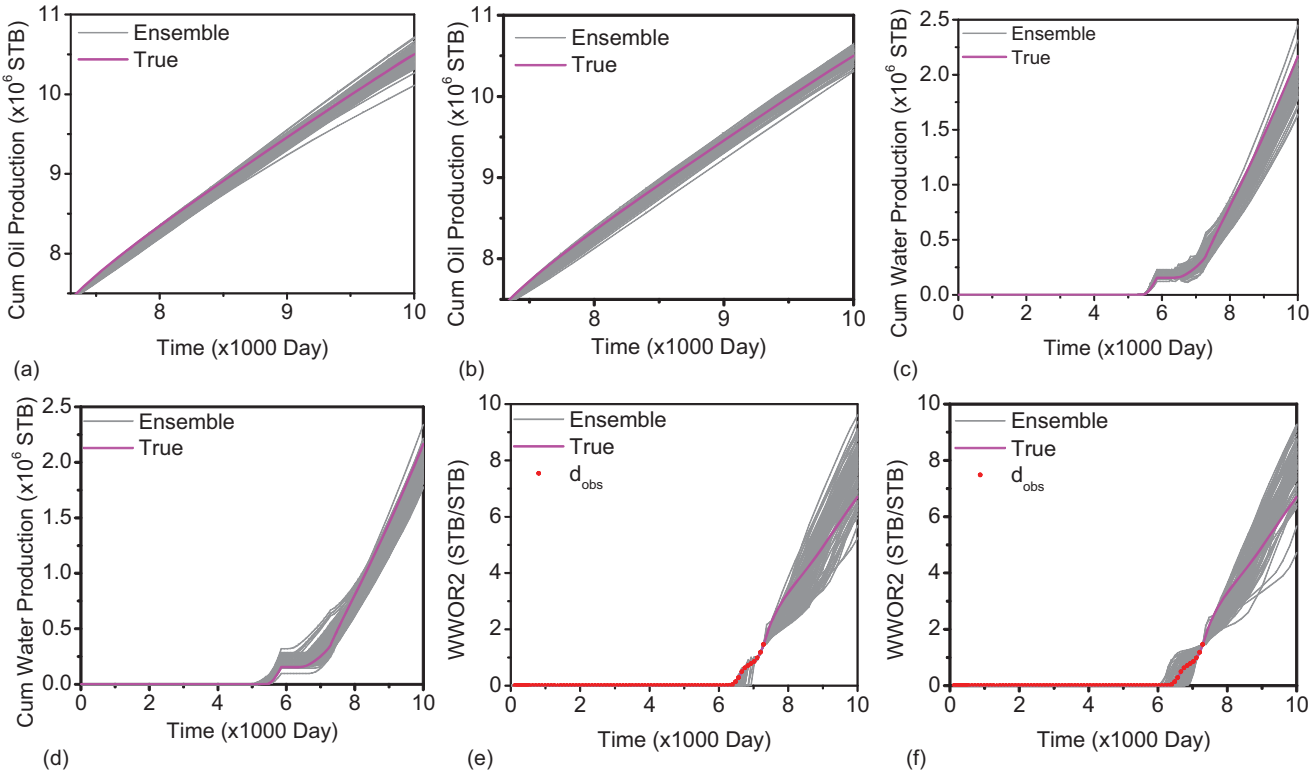


Fig. 4—Production predictions with IEnKF(1) during data assimilation (a, c, and e) and predicted from Time 0 (b, d, and f).

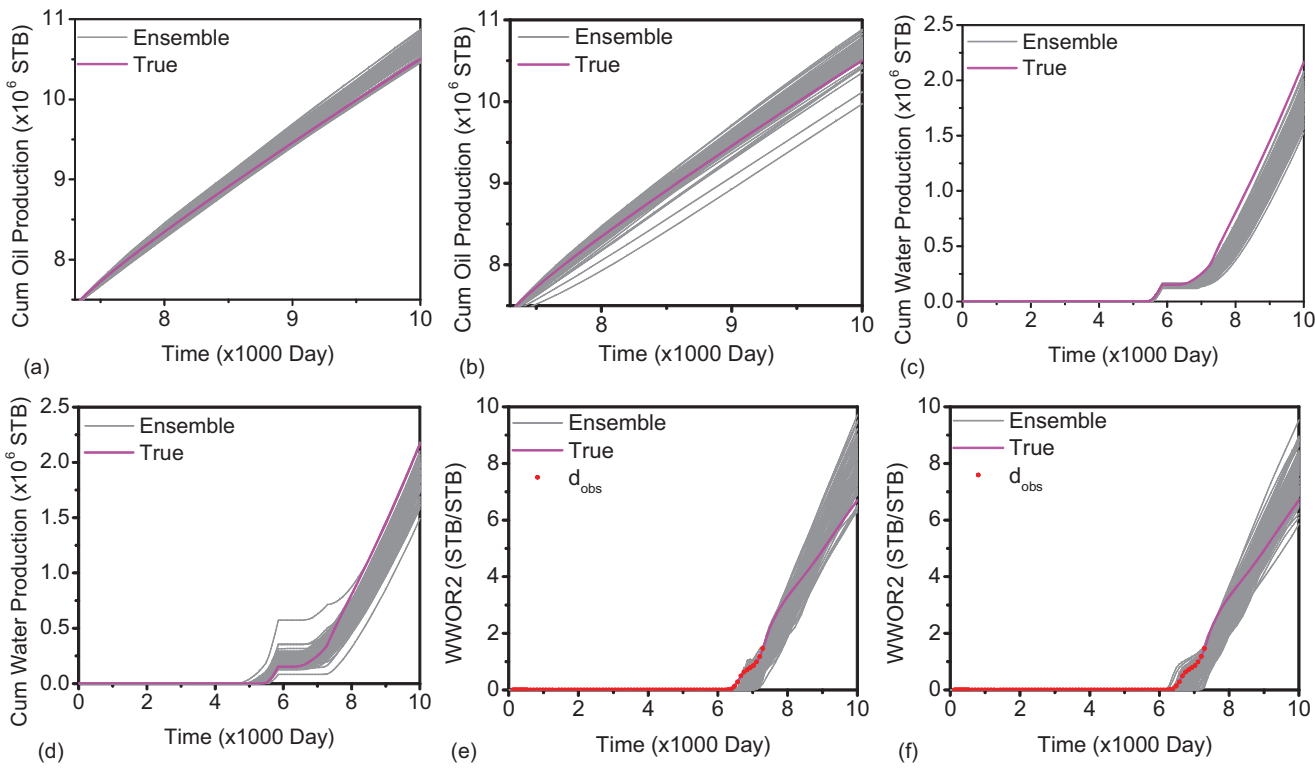


Fig. 5—Production predictions with IEnKF(2) during data assimilation (a, c, and e) and predicted from Time 0 (b, d, and f).

worse than those from IEnKF(1), especially the cumulative water production. Most of the ensemble members underpredict the true cumulative water production. Similar to the results from the IEnKF(1), the match on the water production from Well 5 is good. However, we obtained a relatively poor match of the WOR at Well 2 (Fig. 5e) although the match is far better than that obtained from the standard EnKF. The predictions from time zero with models generated from IEnKF(2) are shown in Figs. 5b, 5d, and 5f.

Conclusions

- The EnKF analysis equations obtained by the “trick” of adding data to the state vector yields proper samples of the marginal pdf we wish to sample under the standard assumption of a Gaussian prior, a Markov dynamical system, and uncorrelated Gaussian measurement errors if the predicted data is linearly related to the state vector of model parameters and dynamical variables. If this linearity assumption is not satisfied, it is not possible to show that EnKF samples correctly.
- When the standard EnKF method fails to give an adequate data match and, as a result, yields poor estimates of future predictions, IEnKF(1) can be applied to obtain an improved match of data and improved predictions.
- Each iteration of IEnKF(1) requires an adjoint solution back to time zero and, thus, requires far more computational time than the standard EnKF method. Because of this, a highly efficient iterative method, IEnKF(2), was developed. Nonexhaustive tests with IEnKF(2) suggest it gives better estimates of future performance predictions than standard EnKF but is far less accurate than IEnKF(1). Whether a more robust iterative method can be formulated that only requires an adjoint solution from the current data assimilation time to the prior data assimilation time is an open question.

Acknowledgments

The support of the member companies of The University of Tulsa Petroleum Reservoir Exploitation Projects (TUPREP) is very gratefully acknowledged.

References

- Bell, B.M. and Cathey, F.W. 1993. The iterated Kalman filter update as a Gauss-Newton method. *IEEE Transactions on Automatic Control* **38** (2): 294–297. DOI: 10.1109/9.250476.
- Brouwer, D.R., Nævdal, G., Jansen, J.-D., Vefring, E.H., and van Kruijsdijk, C.P.J.W. 2004. Improved Reservoir Management Through Optimal Control and Continuous Model Updating. Paper SPE 90149 presented at the SPE Annual Technical Conference and Exhibition, Houston, 26–29 September. DOI: 10.2118/90149-MS.
- Chavent, G., Dupuy, M., and Lemonnier, P. 1975. History Matching by Use of Optimal Control Theory. *SPE J.* **15** (1): 74–86; *Trans., AIME*, **259**. SPE-4627-PA. DOI: 10.2118/4627-PA.
- Chen, W.H., Gavalas, G.R., Seinfeld, J.H., and Wasserman, M.L. 1974. A New Algorithm for Automatic History Matching. *SPE J.* **14** (6): 593–608; *Trans., AIME*, **257**. SPE-4545-PA. DOI: 10.2118/4545-PA.
- Courtier, P., Thépaut, J.-N., and Hollingsworth, A. 1994. A strategy for operational implementation of 4D-Var, using an incremental approach. *The Quarterly Journal of the Royal Meteorological Society* **120** (519): 1367–1387. DOI: 10.1002/qj.49712051912.
- Evensen, G. 2003. The Ensemble Kalman Filter: Theoretical formulation and practical implementation. *Ocean Dynamics* **53** (4): 343–367. DOI: 10.1007/s10236-003-0036-9.
- Evensen, G. 2007. *Data Assimilation: The Ensemble Kalman Filter*. Berlin: Springer Verlag.
- Evensen, G., Hove, J., Meisingset, H.C., Reiso, E., Seim, K.S., and Espelid, S.O. 2007. Using the EnKF for assisted history matching of a north sea reservoir. Paper SPE 106184 presented at the SPE Reservoir Simulation Symposium, Houston, 26–28 February. DOI: 10.2118/106184-MS.
- Eydinov, D., Gao, G., Li, G., and Reynolds, A.C. 2007. Simultaneous estimation of relative permeability curves and porosity/permeability fields by history matching production data. *Proc., 2007 Canadian International Petroleum Conference*, Calgary, 12–14 June.
- Gao, G. 2005. Data Integration and Uncertainty Evaluation for Large Scale Automatic History Matching Problems. Ph.D. thesis, University of Tulsa, Tulsa, Oklahoma.
- Gao, G. and Reynolds A.C. 2006. An Improved Implementation of the LBFGS Algorithm for Automatic History Matching. *SPE J.* **11** (1), 5–17. SPE-90058-PA. DOI: 10.2118/90058-PA.

- Gao, G., Zafari, M., and Reynolds, A.C. 2006. Quantifying Uncertainties for the PUNQ-S3 Problem in a Bayesian Setting With RML EnKF. *SPE J.* **11** (4): 506–515. SPE-93324-PA. DOI: 10.2118/93324-PA.
- Gu, Y. and Oliver, D.S. 2005. History Matching of the PUNQ-S3 Reservoir Model Using the Ensemble Kalman Filter. *SPE J.* **10** (2): 217–224. SPE-89942-PA. DOI: 10.2118/89942-PA.
- Jansen, J.-D., Brouwer, D.R., Nævdal, G., and van Kruijsdijk, C.P.J.W. 2005. Closed-loop reservoir management. *First Break* **23** (January): 43–48.
- Jazwinski, A.H. 1970. *Stochastic Processes and Filtering Theory*. Vol. 64. San Diego, California: Mathematics in Science and Engineering, Academic Press.
- Kalman, R.E. 1960. A new approach to linear filtering and prediction problems. *Transactions of the ASME—Journal of Basic Engineering* **82** (Series D): 35–45.
- Le Dimet, F.-X. and Talagrand, O. 1986. Variational Algorithms for Analysis and Assimilation of Meteorological Observations: Theoretical Aspects. *Tellus* **38A**: 97–110.
- Lewis, J.M. and Derber, J.C. 1985. The use of adjoint equations to solve a variational adjustment problem with advective constraints. *Tellus* **37A**: 309–327.
- Li, G. and Reynolds, A.C. 2007. An Iterative Ensemble Kalman Filter for Data Assimilation. Paper SPE 109808 presented at the SPE Annual Technical Conference and Exhibition, Anaheim, California, USA, 11–14 November. DOI: 10.2118/109808-MS.
- Li, R., Reynolds, A.C., and Oliver, D.S. 2003. History Matching of Three-Phase Flow Production Data. *SPE J.* **8** (4): 328–340. SPE-87336-PA. DOI: 10.2118/87336-PA.
- Nævdal, G., Johnsen, L.M., Aanonsen, S.I., and Vefring, E.H. 2005. Reservoir Monitoring and Continuous Model Updating Using Ensemble Kalman Filter. *SPE J.* **10** (1): 66–74. SPE-84372-PA. DOI: 10.2118/84372-PA.
- Nocedal, J. and Wright, S.J. 1999. *Numerical Optimization*. New York: Springer.
- Oliver, D.S. 1996. On conditional simulation to inaccurate data. *Mathematical Geology* **28** (6): 811–817. DOI: 10.1007/BF02066348.
- Oliver, D.S., He, N., and Reynolds, A.C. 1996. Conditioning permeability fields to pressure data. *Proc.*, 5th European Conference on the Mathematics of Oil Recovery (ECMOR V), Leoben, Austria, 3–6 September, 1–11.
- Oliver, D.S., Reynolds, A.C., and Liu, N. 2008. *Inverse Theory for Petroleum Reservoir Characterization and History Matching*. Cambridge, UK: Cambridge University Press.
- Parrish, D.F. and Derber, J.C. 1992. The National Meteorological Center's Spectral Statistical-Interpolation Analysis System. *Monthly Weather Review* **120**: 1747–1763. DOI: 10.1175/1520-0493(1992)120<1747:TNCSS>2.0.CO;2.
- Reynolds, A.C., He, N., and Oliver, D.S. 1999. Reducing uncertainty in geostatistical description with well testing pressure data. In *Reservoir Characterization: Recent Advances*, ed. R.A. Schatzinger and J.F. Jordan, No. 71, 149–162. Tulsa, Oklahoma: AAPG Memoir, AAPG.
- Reynolds, A.C., Zafari, M., and Li, G. 2006. Iterative Forms of the Ensemble Kalman Filter. *Proc.*, 10th European Conference on the Mathematics of Oil Recovery, Amsterdam, 4–7 September, Paper A030.
- Skjervheim, J.-A., Ruud, B.O., Aanonsen, S.I., Evensen, G., Aanonsen, S.I., and Johansen, T.A. 2006. Using the ensemble Kalman filter with 4D data to estimate properties and Lithology of reservoir rocks. *Proc.*, 10th European Conference on the Mathematics of Oil Recovery, Amsterdam, 4–7 September.
- Thulin, K., Li, G., Aanonsen, S.I., and Reynolds, A.C. 2007. Estimation of Initial Fluid Contacts by Assimilation of Production Data With EnKF. Paper SPE 109975 presented at the SPE Annual Technical Conference and Exhibition, Anaheim, California, USA, 11–14 November. DOI: 10.2118/109975-MS.
- Zafari, M. and Reynolds, A.C. 2007. Assessing the Uncertainty in Reservoir Description and Performance Predictions With the Ensemble Kalman Filter. *SPE J.* **12** (3): 382–391. SPE-95750-PA. DOI: 10.2118/95750-PA.
- Zhang, F. and Reynolds, A.C. 2002. Optimization algorithms for automatic history matching of production data. *Proc.*, 8th European Conference on the Mathematics of Oil Recovery (ECMOR VIII), Frieberg, Germany, 3–6 September, 1–10.
- Zhao, Y., Reynolds, A.C., and Li, G. 2008. Generating Facies Maps by Assimilating Production Data and Seismic Data With the Ensemble Kalman Filter. Paper SPE 113990 presented at the SPE/DOE Symposium on Improved Oil Recovery, Tulsa, 20–23 April. DOI: 10.2118/113990-MS.
- Zhao, Y., Reynolds, A.C., and Li, G. 2008. Generating Facies Maps by Assimilating Production Data and Seismic Data With the Ensemble Kalman Filter. Paper SPE 113990 presented at the SPE/DOE Symposium on Improved Oil Recovery, Tulsa, 20–23 April. DOI: 10.2118/113990-MS.
- Zupanski, M. 2005. Maximum Likelihood Ensemble Filter: Theoretical Aspects. *Monthly Weather Review* **133** (6): 1710–1726. DOI: 10.1175/MWR2946.1.

Gaoming Li is an associate professor in petroleum engineering at The University of Tulsa. He also serves as associate director of TUPREP, an industry research consortium focused on research in reservoir characterization, reservoir simulation, and well testing. His current research interests include reservoir characterization and uncertainty assessment, history matching, and enhanced oil recovery. He holds a BS degree in geophysical well logging and an MS degree in applied geophysics, both from the China University of Petroleum, and a PhD degree in petroleum and natural gas engineering from Pennsylvania State University. **Albert C. Reynolds** is professor of petroleum engineering and mathematics, holder of the McMan Chair in Petroleum Engineering, and Director of TUPREP at The University of Tulsa, where he has been a faculty member since 1970. He has authored or co-authored more than 100 technical papers and two books. His research interests include optimization, assessment of uncertainty, data integration, history matching, and well testing. He holds a BA degree from The University of New Hampshire, an MS degree from Case Institute of Technology, and a PhD degree from Case Western Reserve University, all in mathematics. He received the SPE Reservoir Description and Dynamics Award in 2003, the SPE Formation Evaluation Award in 2005, and became a Distinguished Member in 2001.